tional effect between $W^{\ddagger}_{J}(E - E_0)$ and $\rho_J(E)$. The same is true for the effect of anharmonicity (*6*). Thus, the RRKM calculations were carried out for $J = 0$ and harmonic modes. We present details of these calculations as a function of energy E and for different values of n in Fig. 4.
21. P. J. Stephens, F. J. Devlin, C. F. Chabalowski, M. J. Frisch, *J. Phys. Chem.* **98**, 11623 (1994); G. Rauhut and P. Pulay, *ibid.* **99**, 3093 (1995); A. M. Mebel, K. Morokuma, M. C. Lin, *J. Chem. Phys.* **103**, 7414 (1995); E. W.-G. Diau and S. C. Smith, *ibid.* **106**, 9236 (1997).
22. S. Pedersen, J. L. Herek, A. H. Zewail, *Science* **266**, 1359 (1994); S. K. Kim, J. Guo, J. S. Baskin, A. H. Zewail, *J. Phys. Chem.* **100**, 9202 (1996); S. K. Kim, S. Pedersen, A. H. Zewail, *J. Chem. Phys.* **103**, 477 (1995).
23. The rise of the diradicals and decay of the parent must be related (Fig. 3), and we have detailed the kinetics of the processes involved (E. W.-G. Diau and A. H. Zewail, in preparation). For example, for cyclopentanone and its tetramethyl derivative, the decay of the parent mass is faster than the rise of the diradical mass, indicating a nonconcerted process. By self-consistent analysis of the decay of the parent and the rise of the intermediate, we can obtain the time constants of the elementary steps. Generally, the decay of the parent (or the rise of the intermediate) is the one of relevance here and both the decay and rise are on the femtosecond time scale, independent of n (Fig. 3).
24. A. A. Scala and D. G. Ballan, *Can. J. Chem.* **50**, 3938 (1972); F. H. Dorer, *J. Phys. Chem.* **77**, 954 (1973).
25. R. A. Marcus, in *Picosecond Phenomena III*, K. B. Eisenthal, R. M. Hochstrasser, W. Kaiser, A. Laubereau, Eds. (Springer-Verlag, New York, 1982), pp. 254–259.
26. A. H. Zewail, *Femtochemistry: Ultrafast Dynamics of the Chemical Bond* (World Scientific, Singapore, 1994), and references therein.
27. M. Merchan, B. O. Roos, R. McDiarmid, X. Xing, *J. Chem. Phys.* **104**, 1791 (1996); L. O'Toole, P. Brint, C. Kosmidis, G. Boulakis, P. Tsekeris, *J. Chem. Soc. Faraday Trans.* **87**, 3343 (1991); T. J. Cornish and T. Baer, *J. Am. Chem. Soc.* **109**, 6915 (1987).
28. A. D. Becke, *J. Chem. Phys.* **98**, 5648 (1993).
29. C. Lee, W. Yang, R. G. Parr, *Phys. Rev. B* **37**, 785 (1988).
30. W. Hehre, L. Radom, P. V. R. Schleyer, J. A. Pople, *Ab Initio Molecular Orbital Theory* (Wiley, New York, 1986).
31. S. W. Benson, *Thermochemical Kinetics* (Wiley, New York, ed. 2, 1976).
32. R. G. Gilbert and S. C. Smith, *Theory of Unimolecular and Recombination Reactions* (Blackwell Scientific, Oxford, UK, 1990).
33. S. W. North, D. A. Blank, J. D. Gezelter, C. A. Longfellow, Y. T. Lee, *J. Chem. Phys.* **102**, 4447 (1995).
34. J. Troe, *Ber. Bunsenges. Phys. Chem.* **92**, 242 (1988).
35. Supported by a grant from the Office of Naval Research and by the NSF. We thank R. Bersohn for communicating unpublished results to us and S. Baskin for helpful discussions.

14 October 1997; accepted 5 December 1997

Fluorescent, Sequence-Selective Peptide Detection by Synthetic Small Molecules

Chao-Tsen Chen, Holger Wagner, W. Clark Still*

Small organic sensor molecules were prepared that bind and signal the presence of unlabeled tripeptides in a sequence-selective manner. Sequence-selective peptide binding is a difficult problem because small peptides are highly flexible and there are no clear rules for designing peptide-binding molecules as there are for the nucleic acids. The signaling system involved the application of fluorescence energy transfer and provided large, real-time fluorescence increases (300 to 500 percent) upon peptide binding. With it, these sensors were sensitive enough to detect unlabeled cognate peptides both in organic solution and in the solid state at low micromolar concentrations.

Chemosensors, small molecules that signal the presence of analytes, typically have two components, a receptor site that selectively binds an analyte and a readout mechanism that signals binding (*1*). Receptor components range from simple metal-chelating molecules (*2*) to synthetic host molecules (*3–6*) or, in the case of biosensors, to proteins or protein fragments (*7–9*). By coupling such molecules to a sensitive fluorescent readout system, molecular sensors have been devised for analytes ranging from metal ions to simple organic compounds including monosaccharides (*3*, *4*), creatinine (*5*), aromatic hydrocarbons (*6*), and cyclic adenosine monophosphate (*7*). Here we describe synthetic chemosensors for tripeptides dissolved in the organic solvent chloroform ($CHCl_3$). The chemical structures of our sensors are based on small-molecule peptide-binding receptors that were developed in this laboratory and function as synthetic analogs of the antigen-binding sites of immunoglobulins (*10–16*). For this study we equipped them with a sensitive fluorescence energy transfer (FET) signal transduction system consisting of a fluorophore (**F**) and a quencher (**Q**) that signals binding fluorescently as a result of changes in the average separation of **F** and **Q**. The FET readout used here is a particularly desirable transduction mechanism because of its generality and sensitivity (*17*). Thus, it does not require that the analyte have some special property (for example, be a fluorophore or quencher) other than the ability to cause a conformational change upon binding. As shown in Fig. 1, analyte binding that increases the separation between **F** and **Q** causes enhancement of fluorescence. With the chemosensors described here, enhancements are large enough to be readily visible to the naked eye.

The peptide-binding receptor components of our chemosensors are based on synthetic, amide-linked oligomers of isophthalic acid and cyclic *trans*-1,2-diamine derivatives that are known to provide highly sequence-selective receptors for peptidic substrates (*10–13*, *15*). Such oligomers have structural features that favor peptide binding including (i) conformational restriction (fewer low-energy receptor conformations), (ii) a concave binding site (allows shape-selective substrate binding and significant receptor-substrate contact), and (iii) unassociated hydrogen bond donors and acceptors within or near the binding site (provides spatially localized electrostatic interaction sites that stabilize particular conformations of the receptor-substrate complex). For our isophthalic acid–diamine oligomers, conformational restriction follows from the isophthalic acid and cyclic diamine components that themselves have very limited conformational flexibility and the virtual rigidity of the secondary amide bonds joining them. Although our oligomeric receptors contain multiple amide bonds, the meta substitution of isophthalic acid (benzene-1,3-dicarboxylic acid) and the trans stereochemistry of the diamine components disfavor intramolecular association of hydrogen bond donors and acceptors and thus leave them available for substrate binding. The concave binding site results from the way the oligomers fold.

The particular chemosensors we prepared here are shown in Scheme 1 as **1** and **2**. [Chemosensor **1** is closely related to a previously described receptor (**1** but with CO_2**F** substituted by hydrogen and **Q** substituted by a linker bound to Disperse Red 1) that selectively bound only two tripeptide sequences (D)Pro(L)Val(D)Gln and

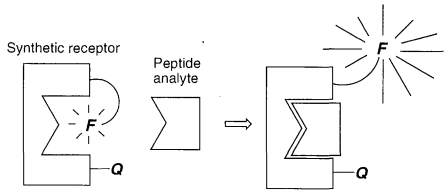

Fig. 1. Analyte binding to the synthetic receptor increases the average separation between ***F*** and ***Q***, resulting in enhanced fluorescence.

Department of Chemistry, Columbia University, New York, NY 10027, USA.

*To whom correspondence should be addressed.

(L)Lys(L)Val(D)Pro from a combinatorial library of 3375 different *N*-acylated, side chain–protected tripeptides (*10*). Chemosensor **2** is a new but related design.

These molecules were synthesized along lines previously described for related receptors lacking fluorescent readout systems (*10*). We will not detail their syntheses here except to note that our chemosensors are amide-linked adducts of macrocyclic tetraamides (compounds **3** and **4**) and the differentially diprotected R,R-diaminopyrrolidine (compound **5**) (Scheme 2). These adducts were functionalized with **Q** as the dabcyl *N*-hydroxysuccinamide ester and with ***F*** as the dansyl sulfonamide of ethanolamine (for **1**) or β-alanine (for **2**). Syntheses and characterization data for **1** and **2** are provided as supplementary material at www.sciencemag.org/feature/data/974405.shl.

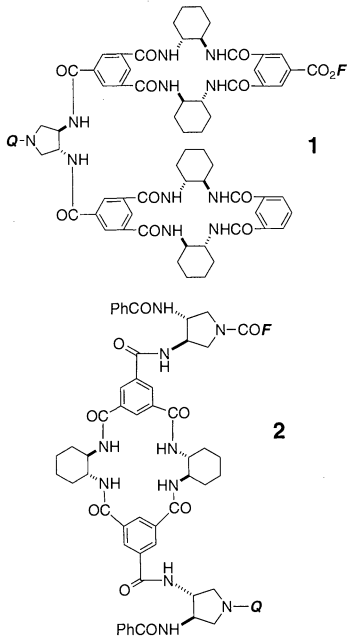

Scheme 1. Functionalized chemosensors **1** and **2**. **Q** is $COC_6H_4N{=}NC_6H_4NMe_2$, and ***F*** is $(CH_2)_2NH\text{-}SO_2C_{10}H_6NMe_2$ (Me, methyl; Ph, phenyl).

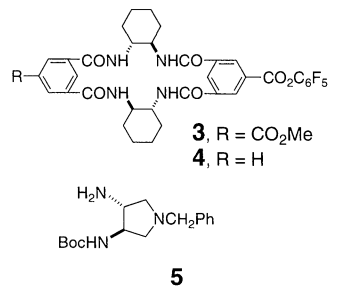

Scheme 2. Synthetic building blocks used for the chemosensors [Boc, $(CH_3)_3COCO$].

To evaluate the peptide-sensing properties of **1** and **2**, we first determined the tripeptide sequences they preferentially bound (cognate peptides) using a previously described solid-phase binding screen with a combinatorial library of 3375 *N*-acetylated, side chain–protected tripeptides in $CHCl_3$ (*18*). This tripeptide library was prepared on Merrifield polystyrene (PS) synthesis beads by the encoded split synthesis method (*19*), resulting in a library of beads in which each bead carried a single tripeptide sequence. The binding screen involved treating the bead library with sensors **1** or **2** (~10 μM in $CHCl_3$) and then selecting and decoding those beads that bound the sensor. In these screens, the binding was detected by simple inspection of the library beads because beads carrying peptides that bound the sensor acquired the orange color of the sensor's dabcyl **Q** moiety. With **1**, the cognate peptides were found to be the same two peptides mentioned above: (D)Pro(L)Val(L)Gln (designated P1) and (L)Lys(L)Val(D)Pro. Thus, **1** selectively binds one tripeptide sequence for every ~1600 sequences in the library at a concentration of 10 μM. Chemosensor **2** was somewhat less selective (binding one tripeptide sequence per ~400 sequences), but it did not bind either of the two tripeptide sequences bound by **1**. Instead, it selectively bound peptides having two L-glutamines flanking a D-amino acid and included (L)Gln(D)Asn(L)Gln (designated P2). Thus, not only was P2 not among the cognate peptides of **1**, but P1 was not among the cognate peptides of **2**. Given these findings, we tested whether **1** would generate a fluorescent signal in the presence of P1 but not with P2, and conversely whether **2** would fluorescently sense P2 but not P1.

We measured the fluorescence of **1** and **2** in the presence and absence of solutions of their cognate peptides (P1 and P2, respectively). The fluorescence spectra (340 nm excitation) of $CHCl_3$ solutions of pure **1** and **2** (~30 μM), respectively, showed 99.6 and 99.0% less fluorescence than dansyl *N*-propylamide under the same conditions and indicated highly effective fluorescence quenching of ***F*** by **Q** in the unbound states. However, adding cognate peptides (P1 and P2 as their *N*-acetyl, C-*n*-propylamides) to **1** and **2** resulted in large fluorescence enhancements (Fig. 2). Thus, with 39 μM **1** in chloroform, the addition of one equivalent of P1 resulted in a >300% increase in fluorescence, whereas 10 equivalents of P1 saturated the chemosensor to give a ~500% total fluorescence increase. With 30 μM **2** and 10 equivalents of P2, the increase was ~100%. Addition of noncognate peptides to **1** or **2** at similar concentrations gave little or no fluorescence enhancement, showing that our chemosensors not only bind peptides at low micromolar concentrations but also discriminate between different peptide sequences. With chemosensor **1**, the discrimination between P1 and P2 was such that no measurable change in fluorescence could be detected when as much as 23 equivalents of noncognate P2 was added. Thus, **1** can detect P1 at concentrations below 1 μM whereas with P2 it provides no detectable fluorescence enhancement even at concentrations 1000 times higher. Chemosensor **2** was less discriminatory but still gave five times the fluorescence with its cognate peptide P2 than with noncognate P1.

The fluorescence increases accompanying binding could also be used to measure the binding constants of the chemosensors with their cognate peptides. Thus, with **1** and P1, a binding constant of 260,000 M^{-1} was found by fluorescence-monitored titration in $CHCl_3$. Other peptides including diastereomeric single point mutations of P1 were bound significantly less tightly. For example, **1** complexed (L)Pro(L)Val(D)Gln with a reduced binding constant of 25,000 M^{-1}, and no binding whatsoever could be detected with **1** and (D)Pro(D)Val(D)Gln. Also, **2** and P2 were significantly bound at low micromolar concentrations although aggregation made it impossible to determine an accurate binding constant.

Given the fluorosensing properties of **1** and **2** in solution, we coupled suitable derivatives of these molecules to solid supports to produce solid-state fluorescent chemosensors that could be studied in real time by fluorescence microscopy. We synthesized hydroxymethylated derivatives of **1** and **2** [where **Q** was $COC_6H_4N{=}NC_6H_4N(Et)\text{-}CH_2CH_2OH$ (Et is ethyl)] and coupling these to 100-μm Merrifield synthesis beads to yield PS-supported chemosensors (PS-1 and PS-2). Intermolecular fluorescence quenching was minimized by using Merrifield synthesis beads having only ~0.03

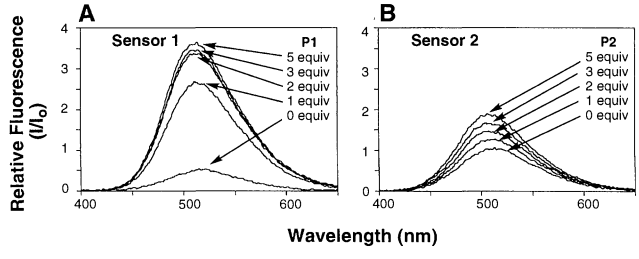

Fig. 2. Fluorescence spectra of chemosensors **1** (39 μM) (**A**) and **2** (30 μM) (**B**) in chloroform titrated by peptides P1 and P2. Equiv, equivalent.

mmol of reactive functionality per gram of beads for immobilization of hydroxymethyl **1** or **2**. Samples of both PS-1 and PS-2 beads were fixed to the bottom of a petri dish and examined with a fluorescence microscope (340 nm excitation and 510 ± 40 nm emission filters). Figure 3A shows the eyepiece view in which PS-1 (slightly greenish) and PS-2 (slightly bluish) fluoresce weakly in the absence of cognate peptides. When P1 is added, however, the fluorescence of PS-1 (but not PS-2) dramatically increases (by ~300%) (Fig. 3B). The enhanced fluorescence of PS-1 can be reduced to its original level by washing with $CHCl_3$, and PS-2 can be made to fluoresce by adding P2 (an increase in fluorescence of 70%) (Fig. 3C). Although low millimolar peptide concentrations could thus be detected visually with PS-1 and PS-2, the more sensitive chemosensor PS-1 could detect P1 concentrations as low as 1 μM by quantitative analysis of a single bead image obtained with the microscope and a charge-coupled device camera.

These experiments demonstrate the sequence-selective optical detection of peptides by a small molecule chemosensor and should be readily extended to biological (and other) sensing applications given recent advances in peptide recognition by synthetic receptors in water (*14*–*16*) and in the preparation of synthetic peptide-binding receptor libraries (*20*). In particular, our simple prescription for peptide-binding small molecules and the ready synthetic accessibility of isophthalic acid–diamine–based receptors clearly indicates one way to make other chemosensing molecules having different peptide-binding properties and selectivities. It should also be straightforward to integrate the methods described here with combinatorial synthesis to prepare solid-state libraries containing many different kinds of chemosensors that could be screened to find compounds having particular sensing properties or used in chemosensing devices incorporating a large, diverse array of selective sensing elements (*21*).

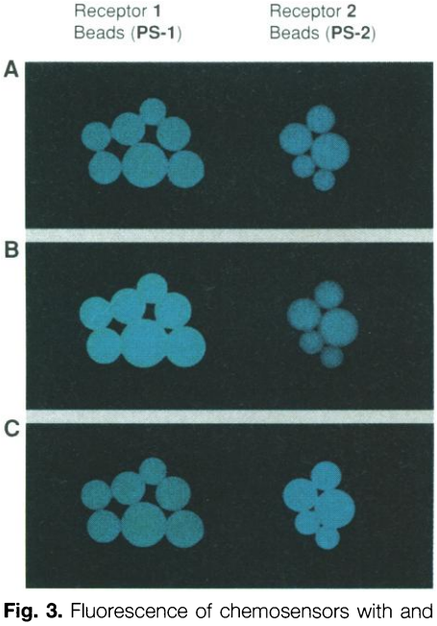

Fig. 3. Fluorescence of chemosensors with and without their cognate peptides: (**A**) absence of peptide, (**B**) presence of 5 mM peptide P1, and (**C**) presence of 5 mM peptide P2.

REFERENCES AND NOTES

1. For reviews, see A. W. Czarnik, *Chem. Biol.* **2**, 423 (1995); L. Fabbrizzi and A. Poggi, *Chem. Soc. Rev.* **1995**, 197 (1995); A. W. Czarnik, Ed., *ACS Symp. Ser. 538* (American Chemical Society, Washington, DC, 1992); J. P. Desvergne and A. W. Czarnik, Eds., *NATO ASI Ser. Ser. C Math Phys. Sci.* (Kluwer, Dordrecht, Netherlands, 1997).
2. R. Y. Tsien, *Biochemistry* **19**, 2396 (1980); M. Kuhn, in *Fluorescent Chemosensors for Ion and Molecule Recognition*, A. W. Czarnik, Ed. (American Chemical Society, Washington, DC, 1993), pp. 147–161.
3. J. Yoon and A. W. Czarnik, *J. Am. Chem. Soc.* **114**, 5874 (1992).
4. T. D. James, K. R. A. Sandanayake, S. Shinkai, *Nature* **374**, 345 (1995).
5. T. W. Bell *et al.*, *Science* **269**, 671 (1995).
6. M. A. Mortellaro and D. G. Nocera, *J. Am. Chem. Soc.* **118**, 7414 (1996); H. Ikeda, M. Nakamura, N. Ise, F. Toda, A. Ueno, *J. Org. Chem.* **62**, 1411 (1997).
7. S. R. Adams, A. T. Harootunian, Y. J. Buechleer, S. S. Taylor, R. Y. Tsien, *Nature* **349**, 694 (1991).
8. G. K. Walkup and B. Imperiali, *J. Am. Chem. Soc.* **118**, 3053 (1996).
9. H. A. Godwin and J. M. Berg, *ibid.*, p. 6514.
10. H. Wennemers, S. S. Yoon, W. C. Still, *J. Org. Chem.* **60**, 1108 (1995).
11. Y. Shao and W. C. Still, *ibid.* **61**, 6086 (1996).
12. Z. Pan and W. C. Still, *Tetrahedron Lett.* **37**, 8699 (1996).
13. E. J. Iorio and W. C. Still, *Bioorg. Med. Chem. Lett.* **6**, 2673 (1996).
14. M. Torneiro and W. C. Still, *J. Am. Chem. Soc.* **117**, 5887 (1995).
15. ———, *Tetrahedron* **53**, 8739 (1997).
16. S. R. LaBrenz and J. W. Kelly, *J. Am. Chem. Soc.* **117**, 3887 (1995); J. S. Albert, M. S. Goodman, A. D. Hamilton, *ibid.*, p. 1143; M. W. Peczuh *et al.*, *ibid.* **119**, 9327 (1997).
17. Intramolecular FET has been used previously to detect metal ion binding [I. Aoki, T. Sakaki, S. Shinkai, *J. Chem. Soc. Chem. Commun.* **1992**, 730 (1992); (*9*)].
18. W. C. Still, *Acc. Chem. Res.* **29**, 155 (1996). The library was supported on polystyrene synthesis beads and included all possible tripeptides (*N*-acetylated and side-chain–protected, 15^3 = 3375 different sequences) from Gly and D- and L-[Ala, Val, Pro, Ser(*O*-tBu), Asn(*N*-Tr), Gln(*N*-Tr), Lys(*N*-Boc)] (Bu, tert-butyl; Tr, trityl).
19. M. H. J. Ohlmeyer *et al.*, *Proc. Natl. Acad. Sci. U.S.A.* **90**, 10922 (1993), and references therein.
20. R. Boyce, G. Li, H. P. Nestler, T. Suenaga, W. C. Still, *J. Am. Chem. Soc.* **116**, 7955 (1994); M. S. Goodman, V. Jubian, B. Linton, A. D. Hamilton, *ibid.* **117**, 11610 (1995); Y. Cheng, T. Suenaga, W. C. Still, *ibid.* **118**, 1813 (1996); H. P. Nestler, *Molity Divers* **2**, 35 (1996).
21. B. G. Healey, S. E. Foran, D. R. Walt, *Science* **269**, 1078 (1995).

22. This work was supported by Multidisciplinary Research Program of the University Research Initiative (Office of Naval Research) grant N00014-95-1-1340 and by a postdoctoral fellowship (to H.W.) from the Deutsche Forschungsgemeinschaft.

13 August 1997; accepted 24 December 1997

Expansion and Length-Dependent Fragility of CTG Repeats in Yeast

Catherine H. Freudenreich, Sara M. Kantrow, Virginia A. Zakian*

Expansion of DNA trinucleotide repeats (TNRs) is the causative mutation in a growing number of human genetic diseases. Large expansions of a CTG tract were obtained and shown by genetic and physical assays to be length-dependent sites of chromosome breakage in *Saccharomyces cerevisiae*. Deletion of *RAD27*, which encodes a nuclease involved in Okazaki fragment processing, caused length-dependent destabilization of CTG tracts and a substantial increase in expansion frequency. The genetic assay described here can be used to evaluate other factors that induce TNR expansion or chromosome fragility in humans.

Expansion of TNRs has been shown to cause human genetic diseases, including myotonic dystrophy, Huntington's disease, several ataxias, and fragile X syndrome (*1*). As a TNR tract expands, the probability of further expansion increases. For example, at the myotonic dystrophy locus, the normal allele size of 5 to 37 CTG/CAG repeats (hereafter called CTG) is relatively stable, but when tracts reach ~50 repeats, they are much more likely to expand in the next generation (*1*). TNR DNA forms stable hairpins that cause replication pausing in vitro (*2*, *3*); it has been proposed that replication pausing promotes expansion or contraction in vivo by replication slippage (*4*). The five known loci of expanded CCG repeats in the human genome all share the additional feature of being fragile sites. Fragile sites, defined as gaps or breaks in condensed human chromosomes, are typically assayed by exposing tissue culture cells to reagents that slow replication or bind

Department of Molecular Biology, Princeton University, Princeton, NJ 08544, USA.

*To whom correspondence should be addressed. E-mail: vzakian@molecular.princeton.edu